Inorganic Chemistry
Article

Inorg. Chem. **2010**, *49*, 5223–5230 **5223**
DOI: 10.1021/ic100337k

Synthesis, Characterization, and Crystal Structures of Silylium Compounds of the Weakly Coordinating Dianion $[B_{12}Cl_{12}]^{2-}$

Mathias Kessler, Carsten Knapp,* Vanessa Sagawe, Harald Scherer, and Rabiya Uzun

Institut für Anorganische und Analytische Chemie, Albert-Ludwigs Universität Freiburg, Albertstrasse 21, 79104 Freiburg i. Br., Germany

Received February 22, 2010

The reaction of $[Ph_3C]_2[B_{12}Cl_{12}]$ with R_3SiH (R = Me, Et, *i*Pr) in 1,2-difluorobenzene yielded the corresponding silylium compounds $(R_3Si)_2B_{12}Cl_{12}$ containing the weakly coordinating dianion $[B_{12}Cl_{12}]^{2-}$. The products were fully characterized by IR and Raman spectroscopy and by multinuclear (^1H, ^{11}B, ^{13}C, ^{29}Si) NMR spectroscopy in solution and the solid state (magic angle spinning). $(Et_3Si)_2B_{12}Cl_{12}$ and $(iPr_3Si)_2B_{12}Cl_{12}$ were characterized by X-ray diffraction. In the solid state, the silylium cations are coordinated to the $[B_{12}Cl_{12}]^{2-}$ anion via silicon−chlorine contacts, which are significantly shorter than the sum of the van der Waals radii. Two different coordination patterns were found. The $[Et_3Si]^+$ cations are coordinated to chlorine atoms of $[B_{12}Cl_{12}]^{2-}$ in the 1 and 12 positions, while the $[iPr_3Si]^+$ cations coordinate to chlorine atoms in the 1 and 7 positions. The 1,12 regioisomer is calculated [for $(Me_3Si)_2B_{12}Cl_{12}$] to be favored over the 1,7 isomer by only 8 kJ mol^{-1}, indicating that packing effects may cause the difference. The silylium cations are very reactive and bind to every Lewis base, being stronger than the aromatic solvent (e.g., benzene, 1,2-difluorobenzene, etc.) used. Consequently, three different crystal structures containing cationic Lewis acid−base complexes $[iPr_3Si\text{-donor}]^+$ were obtained from preparations of $(iPr_3Si)_2[B_{12}Cl_{12}]$. The presence of traces of water leads to crystals of $[iPr_3Si(OH_2)]_2[B_{12}Cl_{12}]$ containing the protonated silanol $[iPr_3Si(OH_2)]^+$, which is only the second example of its kind. Structures containing the $[iPr_3SiOS(H)OSiiPr_3]^+$ cation were obtained from the reaction of $[Ph_3C]_2[B_{12}Cl_{12}]\cdot 2SO_2$ with an excess of iPr_3SiH in 1,2-difluorobenzene. $[iPr_3SiOS(H)OSiiPr_3]_2[B_{12}Cl_{12}]$ and $[iPr_3SiOS(H)OSiiPr_3][(iPr_3Si)B_{12}Cl_{12}]$ were structurally characterized by X-ray diffraction. On the basis of the structural data and quantum chemical calculations, the crystallographically invisible hydrogen atom bound to the sulfur atom was identified. A comparison of the weakly coordinating dianion $[B_{12}Cl_{12}]^{2-}$ with the widely applied corresponding chlorinated carboranes based on several criteria including the ν_{N-H} scale established the dianion $[B_{12}Cl_{12}]^{2-}$ to be as weakly coordinating as the single negatively charged carboranes.

1. Introduction

Not only are silylium cations of academic interest themselves, but they are also very useful starting materials for the synthesis of unusual reactive cations.[1] The quest for a free silylium cation[2] stimulated the research in the field and resulted in the development of several synthetically useful materials containing reactive silylium cations. These have been applied to generate strong alkylating agents[3] and superacids[4] and activate C−F bonds.[5] Silylium compounds are also important starting materials for the synthesis of new and unusual cations and react by silylation or halide subtraction with various substrates. The fast progress in the last 10 years can be mainly attributed to the development and use of very weakly coordinating anions.[6] Very recently, perhalogenated dodecaborate dianions $[B_{12}X_{12}]^{2-}$ (X = F, Cl, Br) were rediscovered and applied as weakly coordinating dianions.[7−9] Improved syntheses for $[B_{12}Cl_{12}]^{2-}$

*To whom correspondence should be addressed. E-mail: carsten.knapp@ac.uni-freiburg.de. Tel: +49-761-203-6150. Fax: +49-761-203-6001.

(1) For review, see: (a) Lambert, J. B.; Zhao, Y.; Zhang, S. M. *J. Phys. Org. Chem.* **2001**, *14*, 370–379. (b) Reed, C. A. *Acc. Chem. Res.* **1998**, *31*, 325–332. (c) Müller, T. *Adv. Organomet. Chem.* **2005**, *53*, 155–215.

(2) Kim, K.-C.; Reed, C. A.; Elliott, D. W.; Mueller, L. J.; Tham, F.; Lin, L.; Lambert, J. B. *Science* **2002**, *297*, 825–827.

(3) Kato, T.; Stoyanov, E.; Geier, J.; Grützmacher, H.; Reed, C. A. *J. Am. Chem. Soc.* **2004**, *126*, 12451–12457.

(4) (a) Stoyanov, E. S.; Hoffmann, S. P.; Juhasz, M.; Reed, C. A. *J. Am. Chem. Soc.* **2006**, *128*, 3160–3161. (b) Küppers, T.; Bernhardt, E.; Eujen, R.; Willner, H.; Lehmann, C. W. *Angew. Chem.* **2007**, *119*, 6462–6465. *Angew. Chem., Int. Ed.* **2007**, *46*, 6346−6349.

(5) (a) Panisch, R.; Bolte, M.; Müller, T. *J. Am. Chem. Soc.* **2006**, *128*, 9676–9682. (b) Douvris, C.; Stoyanov, E. S.; Tham, F. S.; Reed, C. A. *Chem. Commun.* **2007**, 1145–1147. (c) Douvris, C.; Ozerov, O. V. *Science* **2008**, *321*, 1188–1190.

(6) (a) Krossing, I.; Raabe, I. *Angew. Chem.* **2004**, *116*, 2116–2142. *Angew. Chem., Int. Ed.* **2004**, *43*, 2066−2090. (b) Reed, C. A. *Chem. Commun.* **2005**, 1669–1677. (c) Reed, C. A. *Acc. Chem. Res.* **2010**, *43*, 121–128.

(7) Ivanov, S. V.; Miller, S. M.; Anderson, O. P.; Solntsev, K. A.; Strauss, S. H. *J. Am. Chem. Soc.* **2003**, *125*, 4694–4695.

(8) Geis, V.; Guttsche, K.; Knapp, C.; Scherer, H.; Uzun, R. *Dalton Trans.* **2009**, 2687–2694.

(9) Knapp, C.; Schulz, C. *Chem. Commun.* **2009**, 4991–4993.

Published on Web 05/13/2010

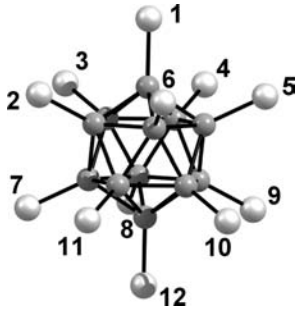

Figure 1. PBE0/def2-TZVPP calculated structure of $[B_{12}Cl_{12}]^{2-}$ and its numbering scheme.

and $[B_{12}F_{12}]^{2-}$ were published,[8,10] and the perhalogenated dodecaborates were applied to synthesize the strong methylating agent $Me_2B_{12}Cl_{12}$[11] and the first diprotic superacid $H_2B_{12}Cl_{12}$.[12] For the latter, the silylium compound $(Et_3Si)_2B_{12}Cl_{12}$ was an important precursor. Thus, silylium cations stabilized by the dodecaborate anion $[B_{12}Cl_{12}]^{2-}$ are important starting materials for the syntheses of reactive compounds.

Herein we present the synthesis and the spectroscopic and structural characterization of silylium cations $[R_3Si]^+$ (R = Me, Et, *i*Pr) stabilized by the perchlorinated weakly coordinating dianion $[B_{12}Cl_{12}]^{2-}$ (Figure 1). The formation of cationic Lewis acid−base complexes in solution and the crystal structures of three examples are discussed as well.

2. Results and Discussion

2.1. $(R_3Si)_2B_{12}Cl_{12}$ (R = Me, Et, *i*Pr). 2.1.1. Synthesis and Spectroscopic Characterization of $(R_3Si)_2B_{12}Cl_{12}$ (R = Me, Et, *i*Pr). Silylium cations are commonly generated by hydride transfer from the corresponding silane to $[Ph_3C]^+$ (trityl) known as the Bartlett−Condon−Schneider hydride transfer reaction (eq 1).[1] The trityl salt $[Ph_3C]_2[B_{12}Cl_{12}]$ is accessible by different routes.[8,12a] It always crystallizes with 2 equiv of solvent molecules. Crystal structures of $[Ph_3C]_2[B_{12}Cl_{12}]\cdot 2D$ with D = $C_2H_4Cl_2$,[8] SO_2,[8] and 1,2-dichlorobenzene[12a] have been characterized.

$$[Ph_3C]_2[B_{12}Cl_{12}] + 2R_3SiH \xrightarrow{1,2\text{-}F_2C_6H_4} (R_3Si)_2B_{12}Cl_{12} + 2Ph_3CH \quad (1)$$

$$R = Me,\ Et,\ iPr$$

The reaction of $[Ph_3C]_2[B_{12}Cl_{12}]$ with silanes R_3SiH (R = Me, Et, *i*Pr) gave the corresponding silylium compounds in good yields. $(Et_3Si)_2B_{12}Cl_{12}$ and $(iPr_3Si)_2B_{12}Cl_{12}$ have some solubility in 1,2-$F_2C_6H_4$ and C_6H_6, while $(Me_3Si)_2B_{12}Cl_{12}$ is only soluble in more polar solvents like liquid SO_2.

The isolated products were characterized by NMR spectroscopy in solution and magic-angle-spinning (MAS) NMR experiments in the solid state. ^{29}Si NMR chemical shifts are indicative of the nature of the silylium cations and the extent of coordination to the counteranion or the solvent. For solid $(R_3Si)_2B_{12}Cl_{12}$, ^{29}Si NMR chemical shifts (R = Me, 118 ppm; R = Et, 126 ppm; R = *i*Pr, 117 ppm) similar to those for the corresponding carborane compounds were found.[13] The observed values are characteristic for silylium cations coordinated by a weakly coordinating anion in the solid state and indicate that under these conditions the basicity of $[B_{12}Cl_{12}]^{2-}$ is similar to that of the very weakly coordinating carborane anions. In solution, characteristic signals of the silylium cations were found as well. The chemical shift in solution reflects interactions between the silylium cation and the solvent and interactions between the silylium cation and the counteranion averaged over time. The $[Et_3Si]^+$ and $[iPr_3Si]^+$ compounds have some solubility in benzene and ^{29}Si NMR chemical shifts in this solvent ($[Et_3Si]^+$, 111 ppm; $[iPr_3Si]^+$, 116 ppm) are in agreement with the previously published data.[1c] The solubility of $(Me_3Si)_2B_{12}Cl_{12}$ in benzene was too low to obtain NMR spectra; therefore, NMR spectra were measured in liquid SO_2. The ^{29}Si NMR chemical shift (88 ppm) was shifted to high field and is in the expected range for a silylium cation in the stronger donor solvent SO_2. In section 2.2.1, the calculated binding strengths of different Lewis bases to $[Me_3Si]^+$ are discussed.

The ^{11}B NMR spectra show a singlet for $[B_{12}Cl_{12}]^{2-}$, indicating the absence of strong bonding between the silylium cations and the anion in solution. In contrast, the bonding of the stronger Lewis acid $[H_3C]^+$ to $[B_{12}Cl_{12}]^{2-}$ in a SO_2 solution leads to splitting of the ^{11}B NMR signal, as was very recently shown for $Me_2B_{12}Cl_{12}$.[11]

2.1.2. Crystal Structures of $(Et_3Si)_2B_{12}Cl_{12}$ and $(iPr_3Si)_2B_{12}Cl_{12}$. Layering of saturated solutions of $(Et_3Si)_2B_{12}Cl_{12}$ and $(iPr_3Si)_2B_{12}Cl_{12}$ in 1,2-difluorobenzene with pentane yielded colorless crystals suitable for X-ray diffraction. The structure determinations revealed that in the solid state strong cation−anion contacts exist and the silylium cations are coordinated to the $[B_{12}Cl_{12}]^{2-}$ anion (Figure 2). In the case of $(Et_3Si)_2B_{12}Cl_{12}$, the silylium cations are bound to the anion in the 1 and 12 positions (see Figure 1 for the numbering scheme).[14] In contrast, a 1,7-coordination mode is found for $(iPr_3Si)_2B_{12}Cl_{12}$. The silicon−chlorine distances [231.75(8)−235.50(12) pm] are significantly shorter than the sum of the van der Waals radii ($\sum$vdW = 390 pm)[15] but are still about 20−25 pm longer than the silicon−chlorine bond length in solid Me_3SiCl [208.63(9) pm].[16] The distances are in the same range as the silicon−chlorine distance in the silylated chloronium cation $[Me_3Si{-}Cl{-}SiMe_3]^+$ [221.5(5)−238.8(5) pm].[17] The relatively strong cation−anion contact results in a lengthening of the boron−chlorine bonds

(10) Peryshkov, D. V.; Popov, A. A.; Strauss, S. H. *J. Am. Chem. Soc.* **2009**, *131*, 18393–18403.
(11) Bolli, C.; Derendorf, J.; Kessler, M.; Knapp, C.; Scherer, H.; Schulz, C.; Warneke, J. *Angew. Chem., Int. Ed.* **2010**, *49*, 3536–3538. *Angew. Chem.* **2010**, *122*, 3616−3619.
(12) (a) Avelar, A.; Tham, F. S.; Reed, C. A. *Angew. Chem.* **2009**, *121*, 3543–3545. *Angew. Chem., Int. Ed.* **2009**, *48*, 3491−3493. (b) Kessler, M.; Knapp, C.; Scherer, H., unpublished results.
(13) Hoffmann, S. P.; Kato, T.; Tham, F. S.; Reed, C. A. *Chem. Commun.* **2006**, 767–769.
(14) The crystal structure of $(Et_3Si)_2B_{12}Cl_{12}$ (crystallized from dichlorobenzene/pentane) has also been reported by Reed et al. in a very recent communication (ref 12a). Despite different space groups, the structures seem to be essentially identical.
(15) Batsanov, S. S. *Inorg. Mater.* **2001**, *37*, 871–885. *Zh. Neorg. Mater.* **2001**, *37*, 1031−1046.
(16) Buschmann, J.; Lentz, D.; Luger, P.; Röttger, M. *Acta Crystallogr., Sect. C: Cryst. Struct. Commun.* **2000**, *C56*, 121–122.
(17) Lehmann, M.; Schulz, A.; Villinger, A. *Angew. Chem.* **2009**, *121*, 7580–7583. *Angew. Chem., Int. Ed.* **2009**, *48*, 7444−7447.

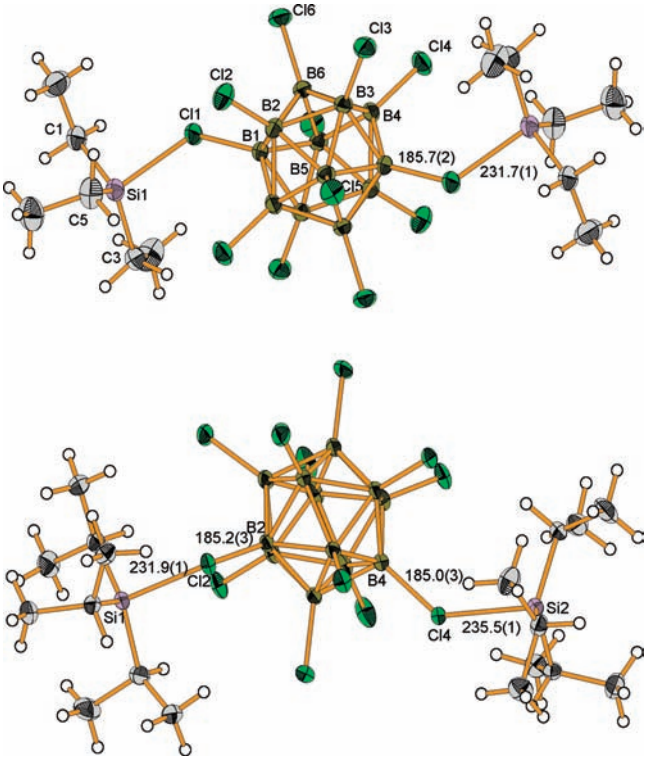

Figure 2. (Top) Crystal structure of $(Et_3Si)_2B_{12}Cl_{12}$. Selected bond lengths [pm] and angles [deg]: Si1−Cl1 231.75(9), Cl1−B1 185.7(2), av. B−Cl 178.6, Si1−Cl1−B1 127.01(8), ∑(C−Si1−C) 347.8. (Bottom) Crystal structure of $(iPr_3Si)_2B_{12}Cl_{12}$. Selected bond lengths [pm] and angles [deg]: Si1−Cl2 231.90(12), Si2−Cl4 235.50(12), Cl2−B2 185.2(3), Cl4−B4 185.0(3), av. B−Cl 178.0, Si1−Cl2−B2 126.97(11), Si2−Cl4−B4 134.11(11), ∑(C−Si1−C) 350.3, ∑(C−Si2−C) 349.2. Thermal ellipsoids are shown at the 50% probability level, and the hydrogen atoms are shown as spheres of arbitrary size.

connected to the silylium cations (av. 185.3 pm) by about 6 pm compared to the free boron−chlorine bonds (av. 178.8 pm). This situation is reminiscent of that found in solid 1,12-$Me_2B_{12}Cl_{12}$ containing two methyl cations coordinated to the $[B_{12}Cl_{12}]^{2-}$ anion.[11] However, the methyl cations are even more strongly bound to the anion, resulting in a carbon−chlorine bond length similar to that of a carbon−chlorine single bond and an even more pronounced lengthening of the boron−chlorine bond. The strength of the cation−anion contacts is also reflected by the sum of the C−Si−C angles around the silicon centers. For an ideal trigonal-planar silylium cation, the sum of the carbon−silicon−carbon angles is 360°. In $(Et_3Si)_2B_{12}Cl_{12}$ (347.8°) and $(iPr_3Si)_2B_{12}Cl_{12}$ (349.2° and 350.3°), these values are reduced by about 10°. The bonding situation in these silylium compounds is identical with that found in the corresponding chlorinated carborane compounds.[13,18] A comparison of the dianion $[B_{12}Cl_{12}]^{2-}$ with the corresponding singly charged carboranes will be given in section 2.3.

Quantum chemical calculations of $(R_3Si)_2B_{12}Cl_{12}$ (R = H, Me) were performed (Table 1) to establish relative energies of the three possible regioisomers (1,12, 1,7, and 1,2; see Figure1 for the numbering scheme) to gain some insight into why two different coordinations were found.

(18) Xie, Z.; Manning, J.; Reed, R. W.; Mathur, R.; Boyd, P. D. W.; Benesi, A.; Reed, C. A. *J. Am. Chem. Soc.* **1996**, *118*, 2922–2928.

Table 1. Calculated [BP86/SV(P)] Relative Energies [kJ mol^{-1}] for the Three Different Regioisomers of $(R_3Si)_2B_{12}Cl_{12}$ (R = H, Me)

isomer	symmetry	relative energies [kJ mol^{-1}]
1,2-$(H_3Si)_2B_{12}Cl_{12}$	C_1	28.9
1,7-$(H_3Si)_2B_{12}Cl_{12}$	C_1	3.6
1,12-$(H_3Si)_2B_{12}Cl_{12}$	C_1	0
1,2-$(Me_3Si)_2B_{12}Cl_{12}$	C_1	28.3
1,7-$(Me_3Si)_2B_{12}Cl_{12}$	C_s	8.0
1,12-$(Me_3Si)_2B_{12}Cl_{12}$	C_{2h}	0

As expected, 1,12 coordination represents the lowest energy isomer, while the 1,2 isomer is about 28 kJ mol^{-1} higher in energy because of the sterical repulsion of the coordinated silylium cations. The energy differences between the 1,12 and 1,7 isomers are rather small (3.6 kJ mol^{-1}, R = H; 8.0 kJ mol^{-1}, R = Me). It can be assumed that the energy difference between the 1,12 and 1,7 isomers increases with the size of the silylium cation; nevertheless, the energy difference for R = iPr_3 seems to be sufficiently small to be overcome by the energy gain of a more efficient packing of the molecules in the crystal lattice.

2.2. Formation of Lewis Acid−Base Complexes. 2.2.1. $[R_3Si\text{-Donor}]^+$ Cations in Solution. In solution, an equilibrium exists between silylium cations coordinated to the anion and silylium cations solvated by the solvent (e.g., benzene or 1,2-difluorobenzene). Every donor present in solution as an impurity and having a higher affinity toward $[R_3Si]^+$ than the solvent (see Table 3) replaces it under the formation of Lewis acid−base complexes, which leads to the appearance of additional signals in the ^{29}Si NMR solution spectra. Depending on the impurities present, various signals in the range from 30 to 80 ppm are observed. The ^{29}Si NMR chemical shifts for the cationic Lewis acid−base complexes are between the typical shifts for neutral trimethlsilyl compounds (ca. 0 ppm) and those for $[R_3Si]^+$ cations in an aromatic solvent (110−120 ppm).[1c] It can be assumed that the additional NMR signals are due to complexes formed with Lewis bases like H_2O, SO_2, and Me_3SiCl, which may be present as an impurity in solution. However, it is impossible to assign the various ^{29}Si NMR signals to certain compounds based on the ^{29}Si NMR chemical shift. To aid in the assignment, ^{29}Si NMR chemical shifts of various neutral and cationic trimethylsilylium species were calculated by the GIAO method, as implemented in the *TURBOMOLE* program. The results, together with calculated and experimental values from the literature, are collected in Table 2. The calculations reproduced previously calculated chemical shifts for $[R_3Si]^+$ cations in the gas phase quite well. Calculated chemical shifts for neutral compounds are in very good agreement with experimental data. Unfortunately, the calculated chemical shifts for the cationic Lewis acid−base complexes $[R_3Si\text{-donor}]^+$ in question are not in very good agreement with experimental data and thus cannot be used to unambiguously assign experimental spectra to a certain compound. For the NMR chemical shift calculations, exactly one donor molecule was added to the free silylium cation. The temperature, concentration, equilibrium in solution, and other solvent effects were not taken into account, showing that the approach currently is still an oversimplification.

Binding energies for the cationic Lewis acid−base complexes were calculated according to eq 2 on the PBE0/TZVPP level (Table 3) to obtain a relative order

Table 2. Comparison of Calculated [PBE0/TZVPP//BP86/SV(P)] and Experimental ^{29}Si NMR Chemical Shifts for Various Neutral Trimethylsilylium Compounds and Corresponding Cations

compound	calcd δ^{29}Si	calcd δ^{29}Si (ref)	exptl δ^{29}Si (ref)
Me_3SiCl	40		30[19]
Me_3SiF	30		32[19]
Me_3SiOH	11		
$Me_3SiOSiMe_3$	3		4[19]
$[Me_3Si]^+$	385	362[a,20]	
$[Et_3Si]^+$	379	371[a,18]	
$[iPr_3Si]^+$	294	342[a,18]	
$[Ph_3Si]^+$	190	199[a,20]	
$[Me_3Si(OSO)]^+$	115		88 (this work)
$[(Me_3Si)_3O]^+$	57	11[a,21]	51[22]
$[Me_3Si(OH_2)]^+$	113		
$[Me_3Si-H-SiMe_3]^+$	109		
$[Me_3Si-Cl-SiMe_3]^+$	108		
$[Me_3Si(C_6H_6)]^+$	97		84[23]
$[Me_3Si(NCCH_3)]^+$	40	38[a,24]	

[a] HF/GIAO.

Table 3. Calculated (PBE0/TZVPP) Binding Energies of Selected Donor Molecules to $[Me_3Si]^+$

donor	calcd (PBE0/TZVPP) binding energy [kJ mol^{-1}]
1,2-$F_2C_6H_4$	−83.9
C_6H_6	−104.0
SO_2	−110.5
Me_3SiH	−131.2
Me_3SiCl	−131.8[a]
H_2O	−147.2
H_3CCN	−208.5

[a] A value of −128.4 kJ mol^{-1} has been calculated on the PBE0/aug-cc-pwCVDZ level in the literature.[17]

of the Lewis base properties of the donor molecules. Exemplarily, calculations were performed for $[Me_3Si]^+$.

$$[Me_3Si]^+ + \text{donor} \xrightarrow{\Delta H} [Me_3Si\text{-donor}]^+ \quad (2)$$

The calculated binding energies are exothermic and range from $\Delta H = -75$ to -199 kJ mol^{-1}. All donor molecules in Table 3 bind stronger to $[Me_3Si]^+$ than the commonly used aromatic solvents benzene and 1,2-difluorobenzene. SO_2, a typical weakly coordinating solvent,[25] turned out to be a stronger donor than the aromatic solvents but is still the weakest donor among the other Lewis bases in Table 3. The calculated binding energies imply that in an aromatic solvent $[Me_3Si]^+$ forms Lewis acid−base complexes with all donor molecules present. Consequently, so far,

Scheme 1

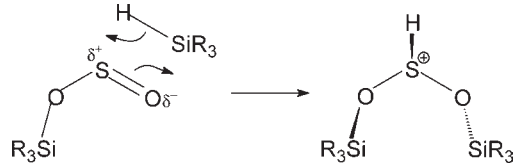

salts containing $[Et_3SiOSO]^+$,[13] $[tBu_3SiOH_2]^+$,[26] $[R_3Si-H-SiR_3]^+$ (R = Me, Et),[12a,13] and $[Me_3Si-X-SiMe_3]^+$ (X = F, Cl, Br, I)[17] cations have been isolated and structurally characterized.

2.2.2. Generation of $[iPr_3SiOH_2]^+$ and $[iPr_3SiOS(H)OSiiPr_3]^+$ Cations. Single crystals of three different byproducts were isolated from the reaction of $[CPh_3]_2[B_{12}Cl_{12}]$ with iPr_3SiH. Traces of water resulted in the formation of $[iPr_3SiOH_2]_2[B_{12}Cl_{12}]$ containing the $[iPr_3SiOH_2]^+$ cation (eq 3).

$$(iPr_3Si)_2[B_{12}Cl_{12}] + 2H_2O \xrightarrow{1,2\text{-}F_2C_6H_4} [iPr_3SiOH_2]_2[B_{12}Cl_{12}] \quad (3)$$

Reactions in the presence of sulfur dioxide yielded crystals of two different compounds. Both seemed to contain a "$[iPr_3SiOSOSiiPr_3]^{n+}$" cation (see section 2.2.4 for a discussion of the structure). The presence of sulfur dioxide can be traced back to the used starting material $[CPh_3]_2[B_{12}Cl_{12}]$, which was washed with SO_2. Because of electric neutrality in the unit cell, the "$[iPr_3SiOSOSiiPr_3]^{n+}$" cations have to have a charge of 1+ only. Quantum chemical calculations and structural data (see section 2.2.4 for a detailed discussion) support the assumption that actually $[iPr_3SiOS(H)OSiiPr_3]^+$ cations possessing a hydrogen atom bonded to the sulfur atom are present (see Scheme 1). The formation of $[iPr_3SiOS(H)OSiiPr_3]^+$ is conceivable by a two-step process. First, a $[R_3SiOSO]^+$ cation is formed (eq 4) by Lewis acid−base adduct formation ($\Delta H = -110.5$ kJ mol^{-1} at the PBE0/TZVPP level for R = Me). Hard electrophiles, e.g., $[R_3Si]^+$, always coordinate to an oxygen atom of SO_2 in a cis manner,[25b,c] and the crystal structure of $[Et_3SiOSO]^+$ is known in the literature.[13] The coordinated SO_2 molecule is polarized, and subsequently a hydrosilylation reaction with an excess of silane (eq 5 and Scheme 1) occurs on the $[R_3SiOSO]^+$ cation ($\Delta H = -233.5$ kJ mol^{-1} for R = Me on the PBE0/TZVPP level). This reaction is reminiscent of the formation of [MeOS(F)OMe][SbF_6] from [MeOSO][SbF_6] and MeF in SO_2 solution.[27]

$$[Ph_3C]_2[B_{12}Cl_{12}]\cdot 2SO_2 + 2iPr_3SiH \xrightarrow{1,2\text{-}F_2C_6H_4} [iPr_3SiOSO]_2[B_{12}Cl_{12}] + 2Ph_3CH \quad (4)$$

$$[iPr_3SiOSO]_2[B_{12}Cl_{12}] + 2iPr_3SiH \xrightarrow{1,2\text{-}F_2C_6H_4} [iPr_3SiOS(H)OSiiPr_3]_2[B_{12}Cl_{12}] \quad (5)$$

(19) Kintzinger, J. P.; Marsmann, H. *NMR Basic Principles and Progress—Oxygen-17 and Silicon-29*; Diehl, P., Fluck, E., Kosfeld, R., Eds.; Springer Verlag: Berlin, 1981.
(20) Müller, T.; Zhao, Y.; Lambert, J. B. *Organometallics* **1998**, *17*, 278–280.
(21) Cypryk, M.; Apeloig, Y. *Organometallics* **1997**, *16*, 5938–5949.
(22) Olah, G. A.; Li, X. Y.; Wang, Q. J.; Rasul, G.; Prakash, G. K. S. *J. Am. Chem. Soc.* **1995**, *117*, 3962–3966.
(23) Lambert, J. B.; Zhang, S. Z.; Ciro, S. M. *Organometallics* **1994**, *13*, 2430–2443.
(24) Arshadi, M.; Johnels, D.; Edlund, U.; Ottosson, C. H.; Cremer, D. *J. Am. Chem. Soc.* **1996**, *118*, 5120–5131.
(25) (a) Waddington, T. C. *Non-Aqueous Solvent Systems*; Academic Press: London, 1965. (b) Mews, R.; Lork, E.; Watson, P. G.; Görtler, B. *Coord. Chem. Rev.* **2000**, *197*, 277–320. (c) Decken, A.; Knapp, C.; Nikiforov, G. B.; Passmore, J.; Rautiainen, J. M.; Wang, X.; Zeng, X. *Chem.—Eur. J.* **2009**, *15*, 6504–6517.
(26) Xie, Z.; Bau, R.; Reed, C. A. *J. Chem. Soc., Chem. Commun.* **1994**, 2519–2520.
(27) Olah, G. A.; Schilling, P.; Bollinger, J. M.; Nishimura, J. *J. Am. Chem. Soc.* **1974**, *96*, 2221–2228.

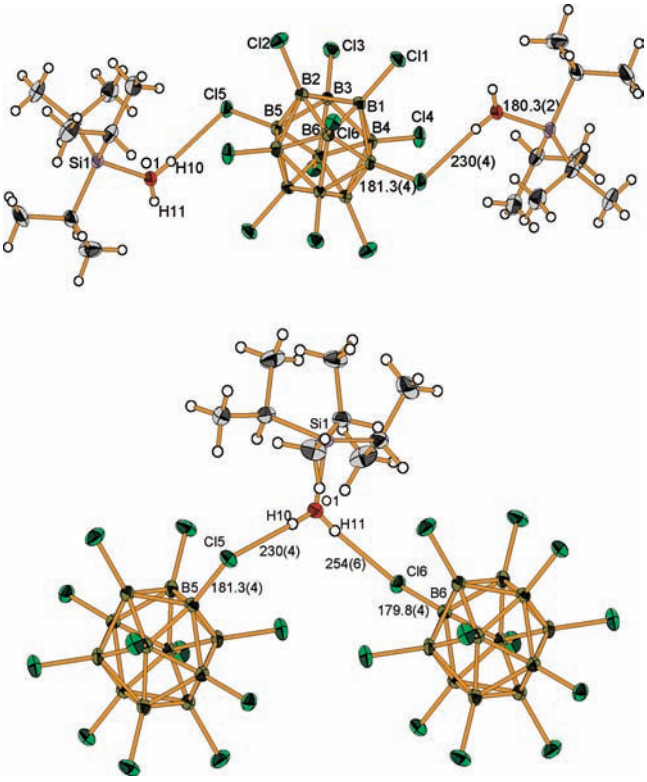

Figure 3. (Top) Crystal structure of $[i\mathrm{Pr_3SiOH_2}]_2[\mathrm{B_{12}Cl_{12}}]$. (Bottom) Coordination sphere of H_2O in $[i\mathrm{Pr_3SiOH_2}]_2[\mathrm{B_{12}Cl_{12}}]$. Selected bond lengths [pm] and angles [deg]: Si1−O1 180.2(3), av. B−Cl 179.5, ∑(C−Si1−C) 346.3. Thermal ellipsoids are shown at the 50% probability level, and the hydrogen atoms are shown as spheres of arbitrary size.

Scheme 2

2.2.3. Crystal Structure of $[i\mathrm{Pr_3SiOH_2}]_2[\mathrm{B_{12}Cl_{12}}]$. Crystallization of $(i\mathrm{Pr_3Si})_2[\mathrm{B_{12}Cl_{12}}]$ from wet 1,2-difluorobenzene/pentane yielded colorless crystals of $[i\mathrm{Pr_3SiOH_2}]_2[\mathrm{B_{12}Cl_{12}}]$ suitable for X-ray diffraction. The obtained structure consists of isolated $[i\mathrm{Pr_3SiOH_2}]^+$ cations and $[\mathrm{B_{12}Cl_{12}}]^{2-}$ anions (Figure 3). $[i\mathrm{Pr_3SiOH_2}]_2[\mathrm{B_{12}Cl_{12}}]$ is only the second example of a structurally characterized protonated silanol. The other example is $[t\mathrm{Bu_3SiOH_2}]^+$ in $[t\mathrm{Bu_3SiOH_2}][\mathrm{CHB_{11}Br_6H_5}]$.[26] The silicon−oxygen distance [180.2(3) pm] is about 15 pm longer than a typical silicon−oxygen single bond (166 pm)[28] and very similar to the silicon−oxygen distance in $[t\mathrm{Bu_3SiOH_2}]^+$ [177.9(9) pm][26] and $[\mathrm{Et_3SiOSO}]^+$ [182.0(5) pm].[13] The weak silicon−oxygen bond is also reflected by a trigonal flattening of the tetracoordinated silicon center. The averaged C−Si−C angle (115.4°; cf. 116.0° in $[t\mathrm{Bu_3SiOH_2}]^+$) lies between that for trigonal-planar (120°) and tetrahedral (109.5°) coordinated centers and is of the same order of magnitude as that in the silylium cations discussed above (see section 2.1.2). The bonding situation in $[i\mathrm{Pr_3SiOH_2}]^+$ is described by a mixture of the two resonance structures in Scheme 2. The left structure represents a silylium cation with a dative Lewis acid−base bond and the right structure an oxonium cation with a covalent silicon−oxygen bond. Quantum chemical calculations show that the positive charge is mainly located on the silicon atom (Paboon charges for $[\mathrm{Me_3SiOH_2}]^+$ on the PBE0/TZVPP level: O, +0.10; Si, +0.57) and suggest a predominance of silylium character.

(28) Huheey, J. E.; Keiter, E. A.; Keiter, R. L. *Anorganische Chemie*, 2nd ed.; de Gruyter: Berlin, 1995.

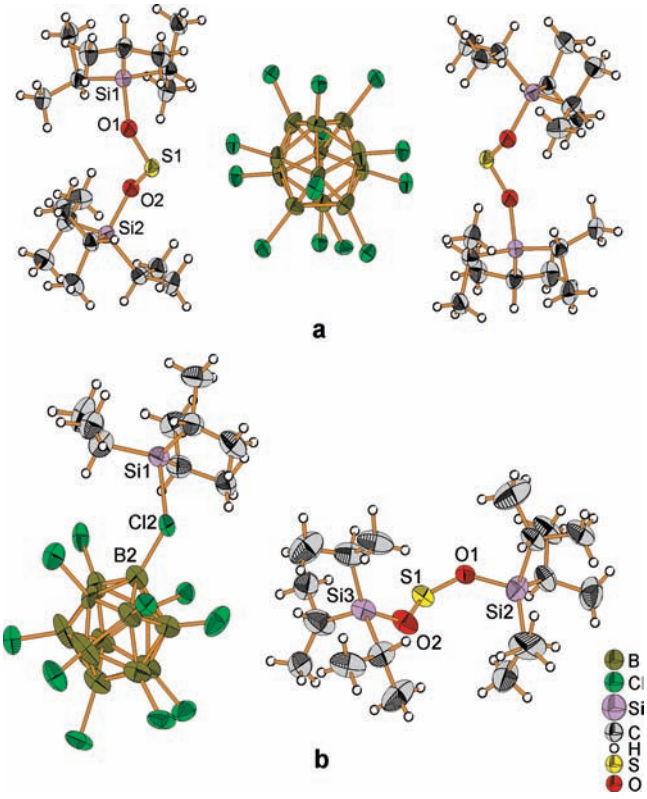

Figure 4. (a) Crystal structure of $[i\mathrm{Pr_3SiOS(H)OSi}i\mathrm{Pr_3}]_2[\mathrm{B_{12}Cl_{12}}]$. Selected bond lengths [pm] and angles [deg]:S1−O1 154.8(5), S1−O2 153.1(6), O1−Si1 178.5(5), O2−Si2 174.4(5), Si1−O1−S1 138.4(4), Si2−O2−S1 124.7(4), O1−S1−O2 105.8(4), ∑(C−Si1−C) 344.1, ∑(C−Si2−C) 342.4, av. Si−C 185.5. (b) Crystal structure of $[i\mathrm{Pr_3SiOS(H)OSi}i\mathrm{Pr_3}][(i\mathrm{Pr_3Si})\mathrm{B_{12}Cl_{12}}]$. Selected bond lengths [pm] and angles [deg]: S1−O1 151.7(9), S1−O2 153.2(8), O1−Si2 171.6(9), O2−Si3 177.5(8), Si2−O1−S1 140.6(7), Si3−O2−S1 131.8(6), O1−S1−O2 112.1(7), ∑(C−Si2−C) 335.9, ∑(C−Si3−C) 338.8, av. Si2−C 185.8, av. Si3−C 185.5, Si1−Cl2 228.8(9), Cl2−B2 186.0(11), Si1−Cl2−B2 125.4(4), ∑(C−Si1−C) 349.2, av. Si1−C 187.0. Thermal ellipsoids are shown at the 30% probability level, and the hydrogen atoms are shown as spheres of arbitrary size. Only the major component of the disordered parts of the structures is shown.

Cations and anions are linked by hydrogen bonds, forming a three-dimensional network. The oxygen−chlorine distances along these bonds are 310 and 327 pm and thus slightly shorter than of the sum of the van der Waals radii (330 pm) and in the typical range for O−H···Cl hydrogen bonds.[28] These weak interactions do not lead to a lengthening of the boron−chlorine bonds involved in hydrogen bonding compared to the others (cf. section 2.1.2).

2.2.4. Crystal Structures of $[i\mathrm{Pr_3SiOS(H)OSi}i\mathrm{Pr_3}]_2[\mathrm{B_{12}Cl_{12}}]$ and $[i\mathrm{Pr_3SiOS(H)OSi}i\mathrm{Pr_3}][(i\mathrm{Pr_3Si})\mathrm{B_{12}Cl_{12}}]$. Colorless crystals suitable for X-ray diffraction of $[i\mathrm{Pr_3SiOS(H)OSi}i\mathrm{Pr_3}]_2[\mathrm{B_{12}Cl_{12}}]$ and $[i\mathrm{Pr_3SiOS(H)OSi}i\mathrm{Pr_3}][(i\mathrm{Pr_3Si})\mathrm{B_{12}Cl_{12}}]$ were obtained from reactions designed to give $(i\mathrm{Pr_3Si})_2\mathrm{B_{12}Cl_{12}}$ in the presence of sulfur dioxide (see section 2.2.2). The crystal structure determinations showed isolated "$[i\mathrm{Pr_3SiOSOSi}i\mathrm{Pr_3}]^{n+}$" cations and $[(i\mathrm{Pr_3Si})\mathrm{B_{12}Cl_{12}}]^-$ or $[\mathrm{B_{12}Cl_{12}}]^{2-}$ anions, respectively (Figure 4).

The OSO bridge and the isopropyl groups in the "$[i\mathrm{Pr_3SiOSOSi}i\mathrm{Pr_3}]^{n+}$" cations are disordered over two sites, which may be explained by the fact that the "OSO" unit can flip from one side to the other. We note that a similar disorder has been observed in the halonium ions $[\mathrm{Me_3Si{-}X{-}SiMe_3}]^+$ (X = F, Cl, Br, I)[17] and in $[\mathrm{Et_3SiOSO}]^+$[13] and thus may be a common feature of cations of this kind. Because of electric neutrality, the "$[i\mathrm{Pr_3SiOSOSi}i\mathrm{Pr_3}]^{n+}$" cations have to have a charge of 1+ only. Quantum chemical calculations of the $[i\mathrm{Pr_3SiOS(H)OSi}i\mathrm{Pr_3}]^+$ cation possessing a hydrogen atom bonded to the sulfur atom resulted in a structure very similar to those observed experimentally [see Figure S15 in the Supporting Information for a comparison of calculated (R = Me) and experimental structures]. For comparison, the structure with the hydrogen atom on oxygen was calculated as well and found to be 47 kJ $\mathrm{mol^{-1}}$ (PBE0/TZVPP) higher in energy. Several quantum chemical studies on the related free acid $\mathrm{H_2SO_2}$ and its isomers have been published.[29] Sulfoxylic acid HOSOH (C_2 symmetry) is about 25 kJ $\mathrm{mol^{-1}}$ lower in energy than sulfinic acid HS(O)OH (C_1 symmetry). Protonation of sulfoxylic acid HOSOH on the sulfur atom to give $[\mathrm{HOS(H)OH}]^+$ is calculated to be favored by 55 kJ $\mathrm{mol^{-1}}$ (PBE0/def2-TZVPP) over protonation on one of the oxygen atoms to give $[\mathrm{HOSOH_2}]^+$. Therefore, it can be concluded that the crystallographically invisible hydrogen atom in "$[i\mathrm{Pr_3SiOS(H)OSi}i\mathrm{Pr_3}]^+$" is located on the sulfur atom. Structural data support this view. The silicon−oxygen bonds are shorter (av. 176 pm; calcd 178 pm) as in $[\mathrm{Et_3SiOSO}]^+$ [182.0(5) pm],[13] and the sulfur−oxygen bonds (av. 153 pm; calcd 154 pm) are lengthened by about 10 pm compared to free $\mathrm{SO_2}$ [gas phase, 143.43(3) pm;[30] solid state, 142.97(7) pm[31]] and correspond to sulfur−oxygen single bonds. This is in contrast to $\mathrm{SO_2}$ molecules bridging two cationic centers (e.g., $\mathrm{Li^+{-}OSO{-}Li^+}$, $\mathrm{Ag^+{-}OSO{-}Ag^+}$),[9,25c] which are almost undistorted with an averaged sulfur−oxygen distance of 142.0 pm. These findings support the structure given in Scheme 1 with single bonds between silicon and oxygen atoms and between oxygen and sulfur atoms and a hydrogen atom on the sulfur atom.

The $[(i\mathrm{Pr_3Si})\mathrm{B_{12}Cl_{12}}]^-$ anion in $[i\mathrm{Pr_3SiOS(H)OSi}i\mathrm{Pr_3}][(i\mathrm{Pr_3Si})\mathrm{B_{12}Cl_{12}}]$ represents the first structurally characterized example of an isolated ion pair $[\text{cation-}\mathrm{B_{12}Cl_{12}}]^-$ in the solid state. A similar strong ion pair $[\mathrm{MeB_{12}Cl_{12}}]^-$ has been suggested to exist in a $\mathrm{SO_2}$ solution. The quality of the structural data due to the extensive disorder prohibits a detailed discussion, but averaged bond lengths in $[(i\mathrm{Pr_3Si})\mathrm{B_{12}Cl_{12}}]^-$ are in good agreement with those in $(i\mathrm{Pr_3Si})_2\mathrm{B_{12}Cl_{12}}$. Attempts to obtain better crystals were unsuccessful.

2.3. Comparison of $[\mathrm{B_{12}Cl_{12}}]^{2-}$ with Related Carboranes. Halogenated carboranes have found various applications in fundamental and applied science and are widely accepted as exceptionally stable and very weakly coordinating anions.[6] In contrast, halogenated dodecaborates have only very recently received attention as weakly coordinating dianions.[8,9,11,12] Therefore, it is of interest to compare the singly negatively charged carboranes and dodecaborates with the 2− charge in terms of their behavior as weakly coordinating anions. Several criteria are available for comparison (Table 4). Reed et al. introduced the $\nu_{\mathrm{N-H}}$ scale,[32] which takes the N−H stretching frequency of $[\mathrm{Oct_3NH}]$[anion] ion pairs in diluted solutions in low polar solvents (e.g., $\mathrm{CCl_4}$, $\mathrm{C_2H_4Cl_2}$) as a measure and already pointed out that based on this scale the dodecaborate and carborane are of similar basicity.[12a] In addition, the structural data of the silylium compounds and the ^{29}Si NMR chemical shift in the benzene solution and the solid state can be compared (Table 4). Neither silicon−chlorine distances nor the sum of the C−Si−C bond angles around the silicon center are significantly different. The same holds for the ^{29}Si NMR chemical shifts.

Therefore, it can be concluded that the basic properties of the chlorinated dodecaborate $[\mathrm{B_{12}Cl_{12}}]^{2-}$ are similarly low for related carborane anions. As a consequence, a chemistry identical with that for the carborane anions[6c] can be expected for the dodecaborates. This becomes attractive because halogenated dodecaborates $[\mathrm{B_{12}X_{12}}]^{2-}$ (X = F, Cl, Br) are much cheaper and easier to prepare than the corresponding carborane anions $[\mathrm{CRB_{11}X_{11}}]^-$ and thus may replace the carboranes for certain applications in the future. However, it should be noted that salts of dodecaborates are usually less soluble because of the higher lattice enthalpy. Nevertheless, there may be cases where it is just desirable to combine the higher lattice enthalpy of the dodecaborate salts with weakly coordinating and weakly basic properties, for instance, for stabilization of reactive dications in the solid state.

3. Experimental Section

General Remarks. Air- and moisture-sensitive solid reagents were manipulated using standard vacuum and Schlenk techniques or in a glovebox with an atmosphere of dry argon ($\mathrm{H_2O}$ and $\mathrm{O_2}$ < 1 ppm). The reactions using liquid sulfur dioxide as a solvent were carried out in H-shaped glass vessels with J. Young Teflon in glass valves and an incorporated fine frit. The solvents liquid sulfur dioxide (Schick), 1,2-difluorobenzene (Fluorochem, 98%), and deuterated solvents (Deutero) were dried over $\mathrm{CaH_2}$ (Merck) and distilled prior to use. *n*-Pentane was purified using a Grubbs solvent purification system. $\mathrm{Et_3SiH}$ (Aldrich, 99%) and $i\mathrm{Pr_3SiH}$ (Aldrich, 99%)[33] are commercially available and were used as received. $[\mathrm{Ph_3C}]_2[\mathrm{B_{12}Cl_{12}}]$,[7] $[\mathrm{Ph_3C}]_2[\mathrm{B_{12}Cl_{12}}]\cdot 2\mathrm{SO_2}$, and $\mathrm{Me_3SiH}$[34] were prepared by published procedures. IR spectra were recorded on a Nicolet Magna-IR 760 equipped with a diamond ATR attachment, and FT-Raman spectra were recorded in flame-sealed capillaries on a Bruker Vertex 70 IR spectrometer equipped with a Bruker RAM II Raman module using a highly sensitive germanium detector and a Nd:YAG laser (1064 nm). ^{1}H, ^{11}B, ^{13}C, and ^{29}Si NMR spectra were measured on a Bruker Avance II WB 400 MHz spectrometer in 5 mm NMR tubes at room temperature with a 5 mm BBFO probe head. Chemical shifts are given with respect to $\mathrm{Me_4Si}$ (^{1}H, ^{13}C, and ^{29}Si) and $\mathrm{BF_3\cdot OEt_2}$ (^{11}B). Spectra measured in liquid sulfur dioxide as a solvent were measured unlocked. Two-dimensional HSQC and

(29) (a) Frank, A. J.; Sadílek, M.; Ferrier, J. G.; Tureček, F. *J. Am. Chem. Soc.* **1996**, *118*, 11321–11322. (b) Otto, A. H.; Steudel, R. *Eur. J. Inorg. Chem.* **2000**, 617–624. (c) Napolion, B.; Huang, M.-J.; Watts, J. D. *J. Phys. Chem. A* **2008**, *112*, 4158–4164.

(30) Holder, C. H.; Fink, M. *J. Chem. Phys.* **1981**, *75*, 5323.

(31) Cited in ref 25b as:Buschmann, J.; Steudel, R., unpublished results.

(32) Stoyanov, E. S.; Kim, K.-C.; Reed, C. A. *J. Am. Chem. Soc.* **2006**, *128*, 8500–8508.

(33) The $i\mathrm{Pr_3SiH}$ should be checked for purity by ^{1}H NMR. Commercially available $i\mathrm{Pr_3SiH}$ from Acros (98%) was found to contain a mixture of *i*Pr and *n*Pr groups.

(34) Tannebaum, S.; Kaye, S.; Lewenz, G. F. *J. Am. Chem. Soc.* **1953**, *75*, 3753–3757.

Table 4. Comparison of the Structural and Spectroscopic Parameters of Silylium Compounds of $[B_{12}Cl_{12}]^{2-}$ and $[CHB_{11}H_{5-x}Cl_{6+x}]^{-}$ (x = 0, 5)

	d(Si−Cl) [pm]	d(Cl−B)[a] [pm]	α(Si−Cl−B) [deg]	∑α(C−Si−C) [deg]	^{29}Si NMR (C_6D_6) [ppm]	^{29}Si NMR MAS [ppm]	ν_{N-H}[b]($C_2H_4Cl_2$) [cm^{-1}]
$(Et_3Si)_2B_{12}Cl_{12}$	231.75(8)	185.6(2)	127.02(7)	347.8	111	126	3154
$(iPr_3Si)_2B_{12}Cl_{12}$	231.90(12)	185.2(3)	126.97(11)	350.3	116	117	
	235.50(12)	185.0(3)	134.11(11)	349.2			
$(iPr_3Si)_2CHB_{11}H_5Cl_6$[18]	232.3(3)	188(1)	122.6(3)	351.8	103[13]	115[18]	3180[6]
$(Et_3Si)_2CHB_{11}Cl_{11}$[13]	233.44(3)	184.12(9)	124.36(3)	349.5	N/A	N/A	3178[6]

[a] Refers to the chlorine atom, which is bonded to the silylium cation. [b] Refers to the N−H stretching frequency of the [Oct_3NH][anion] ion pair in a diluted $C_2H_4Cl_2$ solution.[32]

Table 5. Crystallographic Data for $(Et_3Si)_2B_{12}Cl_{12}$, $(iPr_3Si)_2B_{12}Cl_{12}$, $[iPr_3SiOH_2]_2[B_{12}Cl_{12}]$, $[iPr_3SiOS(H)OSiiPr_3]_2[B_{12}Cl_{12}]$, and $[iPr_3SiOS(H)OSiiPr_3][(iPr_3Si)B_{12}Cl_{12}]$

	$(Et_3Si)_2B_{12}Cl_{12}$[14]	$(iPr_3Si)_2B_{12}Cl_{12}$	$[iPr_3SiOH_2]_2[B_{12}Cl_{12}]$	$[iPr_3SiOS(H)OSiiPr_3]_2$-$[B_{12}Cl_{12}]$	$[iPr_3SiOS(H)OSiiPr_3]$-$[(iPr_3Si)B_{12}Cl_{12}]$
empirical formula	$C_{12}H_{30}B_{12}Cl_{12}Si_2$	$C_{18}H_{42}B_{12}Cl_{12}Si_2$	$C_{18}H_{46}B_{12}Cl_{12}O_2Si_2$	$C_{36}H_{86}B_{12}Cl_{12}O_4S_2Si_4$	$C_{27}H_{63}B_{12}Cl_{12}O_2SSi_3$
M/g mol^{-1}	785.66	869.82	905.85	1314.65	1091.22
cryst syst	monoclinic	monoclinic	monoclinic	monoclinic	monoclinic
space group	$P2_1/c$	$P2_1/c$	$C2/c$	$P2_1/n$	$P2_1$
a/pm	920.10(18)	1065.2(2)	2898.3(6)	1349.0(3)	1381.4(3)
b/pm	1953.3(4)	1558.4(3)	895.18(18)	1287.0(3)	1199.3(2)
c/pm	1286.6(4)	2403.4(5)	1882.8(4)	1912.0(4)	1592.2(3)
β/deg	132.023(18)	96.40(3)	120.94(3)	94.52(3)	92.37(3)
V/nm^3	1.7178(9)	3.9649(14)	4.1899(19)	3.3092(13)	2.6355(9)
Z	2	4	4	2	2
δ_{calcd} /g cm^{-3}	1.519	1.457	1.436	1.319	1.375
θ range/deg	3.04−27.48	3.01−27.48	3.10−25.00	3.03−24.00	3.01−24.00
T/K	203(2)	113(2)	113(2)	100(2)	113(2)
μ/mm^{-1}	1.047	0.915	0.872	0.672	0.766
reflns collected	24 973	28 809	27 683	31 420	33 585
indep reflns	3925 [R_{int} = 0.0625]	8022 [R_{int} = 0.0314]	3680 [R_{int} = 0.0996]	5189 [R_{int} = 0.1469]	8245 [R_{int} = 0.0383]
R1, wR2 [$I > 2\sigma(I)$][a]	0.0360, 0.0646	0.0361, 0.1076	0.0384, 0.0711	0.0732, 0.1744	0.0535, 0.1422
R1, wR2 (all data)	0.0542, 0.0694	0.0480, 0.1372	0.0611, 0.0761	0.1296, 0.2050	0.0746, 0.1609
largest diff peak and hole	0.372, −0.270	0.767, −0.776	0.436, −0.428	0.470, −0.363	0.296, −0.254

[a] R1 = $\sum||F_o| - |F_c||/\sum|F_o|$, wR2 = $(\sum[w(F_o^2 - F_c^2)^2]/\sum[wF_o^4])^{1/2}$.

HMBC experiments were carried out to obtain ^{13}C and ^{29}Si NMR chemical shifts and J_{C-H} coupling constants. MAS NMR experiments were performed on the same spectrometer with a 4 mm CP-MAS probe head. One-pulse experiments were carried out with varying sample spinning rates between 0 and 15 kHz. ^{1}H and ^{29}Si MAS NMR spectra were referenced to hexamethyldisiloxane [HDMSO; δ (^{1}H) = 0, δ (^{29}Si) = 6]. All actual spectra are included with the Supporting Information.

$(Me_3Si)_2B_{12}Cl_{12}$. $[Ph_3C]_2[B_{12}Cl_{12}]$ (0.72 g, 0.69 mmol) was charged into a double Schlenk flask and dissolved in 10 mL of 1,2-$F_2C_6H_4$. Me_3SiH (0.55 g, 7.44 mmol) was added at −196 °C, and the reaction mixture was stirred for 1.5 h at 0 °C. A total of 10 mL of pentane was added, and a white precipitate formed, which was separated by filtration through a fine frit and washed with pentane. Removal of all volatiles in a vacuum yielded $[Me_3Si]_2B_{12}Cl_{12}$ as a white solid (0.38 g, 0.54 mmol, 78%). ^{1}H NMR (400.17 MHz, SO_2, unlocked, 298 K): δ 0.46 (s, 9H, CH_3). ^{11}B NMR (128.39 MHz, SO_2, unlocked, 298 K): δ −11.4. ^{13}C (100.63 MHz, SO_2, unlocked, 298 K): δ 1.2 (CH_3, $^1J_{C-H}$ = 123 Hz). ^{29}Si NMR (79.5 MHz, SO_2, unlocked, 298 K): δ 87.7 $[Me_3Si(SO_2)]^+$. ^{1}H MAS NMR (400.17 MHz, spinning rate 8 kHz, referenced to HDMSO, 298 K): δ 0.9 (CH_3). ^{11}B MAS NMR (128.39 MHz, spinning rate 8 kHz, unreferenced, 298 K): δ −9.5. ^{29}Si MAS NMR (79.5 MHz, spinning rate 8 kHz, referenced to HDMSO, 298 K): δ 117.8 $[Me_3Si]^+$. IR (cm^{-1}): ν 3184 (vw), 1604 (br), 1506 (m), 1453 (vw), 1265 (s), 1207 (vw), 1030 (vs) $[B_{12}Cl_{12}]^{2-}$, 865 (sh), 839 (s), 821 (s), 763 (m), 699 (w), 642 (m), 624 (sh), 530 (vs) $[B_{12}Cl_{12}]^{2-}$. Raman (cm^{-1}) ν 3061(10), 2938(20), 2905(40), 2757(30), 1604(30), 990(10), 764(10), 624(20), 300(100) $[B_{12}Cl_{12}]^{2-}$, 126(40) $[B_{12}Cl_{12}]^{2-}$.

$(Et_3Si)_2B_{12}Cl_{12}$. $[Ph_3C]_2[B_{12}Cl_{12}]$ (0.33 g, 0.32 mmol) was charged into a double Schlenk flask and dissolved in 5 mL of 1,2-$C_6H_4F_2$. Et_3SiH (0.36 g, 3.13 mmol) was added at 0 °C, and the reaction mixture was stirred for 1.5 h. A total of 5 mL of pentane was added, and a white precipitate formed, which was separated by filtration through a fine frit and washed with pentane. Removal of all volatiles in a vacuum yielded $[Et_3Si]_2B_{12}Cl_{12}$ as a white solid (0.15 g, 0.19 mmol, 62%). ^{1}H NMR (400.17 MHz, benzene-d_6, 298 K): δ 0.66 (t, 9H, CH_3), 0.96 (q, 6H, CH_2). ^{11}B NMR (128.39 MHz, benzene-d_6, 298 K): δ −11.3. ^{13}C (100.63 MHz, benzene-d_6, 298 K): δ 5.6 (CH_3, $^1J_{C-H}$ = 129 Hz), 8.5 (CH_2, $^1J_{C-H}$ = 124 Hz). ^{29}Si NMR (79.5 MHz, benzene-d_6, 298 K): δ 111.3 $[Et_3Si(\text{benzene-}d_6)]^+$. ^{1}H MAS NMR (400.17 MHz, spinning rate 10 kHz, referenced to HDMSO, 298 K): δ 1.2 (CH_2CH_3). ^{11}B MAS NMR (128.39 MHz, spinning rate 10 kHz, unreferenced, 298 K): δ −10.4. ^{29}Si MAS NMR (79.5 MHz, spinning rate 10 kHz, unreferenced, 298 K): δ 125.6 $[Et_3Si]^+$. IR (cm^{-1}): ν 2964 (m), 2940 (sh), 2881 (m), 1619 (br), 1457 (m), 1406 (w), 1384 (sh), 1248 (m), 1127 (sh), 1030 (vs) $[B_{12}Cl_{12}]^{2-}$, 748 (s), 688 (s), 678 (s), 534 (vs) $[B_{12}Cl_{12}]^{2-}$, 513 (s). Raman (cm^{-1}) ν 2979(10), 2941(20), 2921(15), 2883(50), 2755(5), 1467(5), 1404(5), 1003(5), 978(5), 575(20), 300(100) $[B_{12}Cl_{12}]^{2-}$, 127(60) $[B_{12}Cl_{12}]^{2-}$.

$(iPr_3Si)_2B_{12}Cl_{12}$. $[Ph_3C]_2[B_{12}Cl_{12}]$ (0.32 g, 0.31 mmol) was charged into a double Schlenk flask and dissolved in 5 mL of 1,2-$C_6H_4F_2$. iPr_3SiH (0.31 g, 1.96 mmol) was added at 0 °C, and the reaction mixture was stirred for 1.5 h. A total of 5 mL of pentane was added, and a white precipitate formed, which was separated by filtration through a fine frit and washed with pentane. Removal of all volatiles in a vacuum yielded $[iPr_3Si]_2B_{12}Cl_{12}$ as a white solid (0.17 g, 0.20 mmol, 63%). ^{1}H NMR (400.17 MHz, benzene-d_6, 298 K): δ 0.68 (d, 18H, CH_3), 0.92 (m, 3H, CH). ^{11}B NMR (128.39 MHz, benzene-d_6, 298 K): δ −11.3. ^{13}C (100.63 MHz, benzene-d_6, 298 K): δ 17.3 (CH_3, $^1J_{C-H}$ = 127 Hz), 17.6 (CH, $^1J_{C-H}$ = 122 Hz). ^{29}Si NMR (79.5 MHz, benzene-d_6, 298 K): δ 115.8 $[iPr_3Si(\text{benzene-}d_6)]^+$. ^{1}H MAS NMR (400.17 MHz, spinning

rate 10 kHz, referenced to HDMSO, 298 K): δ 0.9 ($CH(CH_3)_2$). ^{11}B MAS NMR (128.39 MHz, spinning rate 10 kHz, unreferenced, 298 K): δ −9.5. ^{29}Si MAS NMR (79.5 MHz, spinning rate 10 kHz, referenced to HDMSO, 298 K): δ 116.8 [iPr$_3$*Si*]$^+$. IR (cm^{-1}): ν 2949 (w), 2871 (w), 1461 (m), 1029 (vs) $[B_{12}Cl_{12}]^{2-}$, 882 (s), 696 (m), 656 (sh), 533 (s) $[B_{12}Cl_{12}]^{2-}$. Raman (cm^{-1}) ν 2936(20), 2871(30), 2759(40), 1504(50), 882(50), 299(100) $[B_{12}Cl_{12}]^{2-}$, 127(20) $[B_{12}Cl_{12}]^{2-}$.

[*i*Pr$_3$SiOS(H)OSi*i*Pr$_3$]$_2$[B$_{12}$Cl$_{12}$] and [*i*Pr$_3$SiOS(H)OSi*i*Pr$_3$][(*i*Pr$_3$Si)B$_{12}$Cl$_{12}$]. [iPr$_3$SiOS(H)OSiiPr$_3$]$_2$[$B_{12}Cl_{12}$] and [iPr$_3$SiOS(H)OSiiPr$_3$][(iPr$_3$Si)$B_{12}Cl_{12}$] were obtained from the reaction of $[Ph_3C]_2[B_{12}Cl_{12}]\cdot 2SO_2$ with an excess of iPr$_3$SiH in 1,2-difluorobenzene. Single crystals suitable for X-ray diffraction were prepared by layering the solution with pentane. Attempts to obtain a pure bulk sample or better single crystals were unsuccessful.

X-ray Crystallography. Single crystals suitable for X-ray diffraction were prepared by layering a solution of the corresponding compound in 1,2-difluorobenzene with pentane. Single-crystal X-ray structure determinations were carried out on a Rigaku R-AXIS Spider image plate diffractometer using Mo K_α (0.710 73 Å) radiation. The crystals were mounted onto a kryo loop using fluorinated oil and frozen in the cold nitrogen stream of the goniometer. Details of the crystallographic data collection and refinement parameters are given in Table 5. The structures were solved by direct methods (*SHELXS*).[35] Subsequent least-squares refinement on F^2 (*SHELXL*) located the positions of the remaining atoms in the electron density maps.[35] All atoms were refined anisotropically. Hydrogen atoms were placed in calculated positions using a riding model and were refined isotropically in blocks except for hydrogen atoms bonded to oxygen or sulfur, which were located from the difference Fourier map. The data were corrected for absorption (semiempirical from equivalents). Graphical representations of the structures were prepared with the program *Diamond*.[36] The disordered structures of [iPr$_3$SiOS(H)OSiiPr$_3$]$_2$[$B_{12}Cl_{12}$] and [iPr$_3$SiOS(H)OSiiPr$_3$][iPr$_3$Si][$B_{12}Cl_{12}$] were modeled over two sites using restraints. Chlorine atoms were modeled over two positions, while only one averaged position was refined for the boron atoms. This results in either too short or too long boron−chlorine distances.

Quantum Chemical Calculations. Density functional theory (BP86 and PBE0) calculations were performed with SV(P) and TZVPP basis sets, as implemented in the program *TURBOMOLE*.[37] Frequency calculations were calculated analytically with the AOFORCE module at the same level for all species.[38] All calculated species are true minima on the energy hypersurface, as shown by the absence of imaginary frequencies. Calculations of NMR chemical shifts were performed with the MPSHIFT module.[39] Calculated coordinates and total energies are included with the Supporting Information.

Acknowledgment. The authors are grateful to Prof. Dr. Ingo Krossing for support and helpful discussions and Boumahdi Benkmil for assistance with the X-ray diffraction measurements. This work was supported by the Albert-Ludwigs Universität Freiburg and the Deutsche Forschungsgemeinschaft.

Supporting Information Available: Crystallographic data in CIF format for $(Et_3Si)_2B_{12}Cl_{12}$, (iPr$_3$Si)$_2$$B_{12}Cl_{12}$, [$iPr_3$SiOH$_2$]$_2$-[$B_{12}Cl_{12}$], [$iPr_3$SiOS(H)OSi$iPr_3$]$_2$[$B_{12}Cl_{12}$], and [$iPr_3$SiOS(H)-OSi$iPr_3$][($iPr_3$Si)$B_{12}Cl_{12}$], actual NMR and vibrational spectra, and calculated absolute energies, symmetries, and coordinates for all calculated species. This material is available free of charge via the Internet at http://pubs.acs.org.

(35) Sheldrick, G. M. *SHELX-97: Programs for Crystal Structure Analysis*, release 97-2; Institut für Anorganische Chemie der Universität Göttingen: Göttingen, Germany, **1997**.

(36) *Diamond—Crystal and Molecular Structure Visualization*, version 3.2e, **1997−2010**, Crystal Impact - K. Brandenburg & H. Putz GbR, Rathausgasse 30, D-53111 Bonn.

(37) *TURBOMOLE*, version 6.1, **2009**, a development of University of Karlsruhe and Forschungszentrum Karlsruhe GmbH, 1989−2007, TURBOMOLE GmbH, since 2007; available from http://www.turbomole.com.

(38) Deglmann, P.; Furche, F.; Ahlrichs, R. *Chem. Phys. Lett*. **2002**, *362*, 511–518.

(39) Schreckenbach, G.; Ziegler, T. *J. Phys. Chem*. **1995**, *99*, 606–611.